ORIGINAL RESEARCH

Aberrant Epithelial Differentiation Contributes to Pathogenesis in a Murine Model of Congenital Tufting Enteropathy

Barun Das,[1] Kevin Okamoto,[1] John Rabalais,[1] Jocelyn A. Young,[1,2] Kim E. Barrett,[3] and Mamata Sivagnanam[1,2]

[1]Department of Pediatrics, University of California, San Diego, La Jolla, California; [2]Department of Pediatrics, Rady Children's Hospital, San Diego, California; and [3]Department of Medicine, University of California, San Diego, La Jolla, California
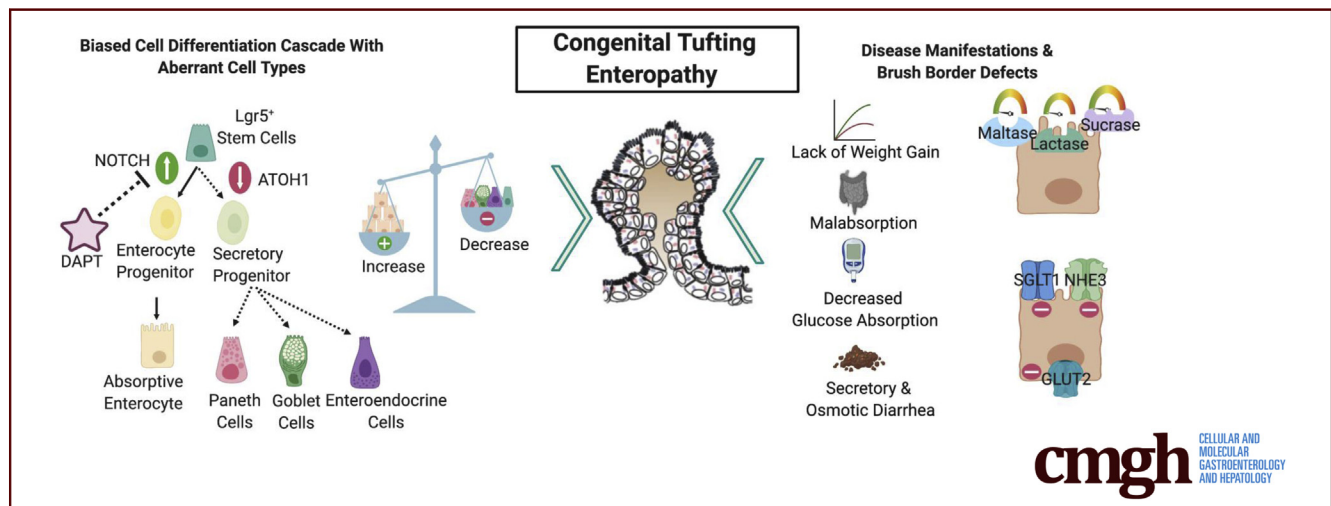
SUMMARY

A murine model of congenital tufting enteropathy exhibits altered intestinal cell differentiation, leading to increased absorptive and decreased major secretory cells, which can be reversed with DAPT. Absorptive enterocytes in these mice are also dysfunctional, contributing to disease pathogenesis.

BACKGROUND & AIMS: Congenital tufting enteropathy (CTE) is an intractable diarrheal disease of infancy caused by mutations of epithelial cell adhesion molecule (EpCAM). The cellular and molecular basis of CTE pathology has been elusive. We hypothesized that the loss of EpCAM in CTE results in altered lineage differentiation and defects in absorptive enterocytes thereby contributing to CTE pathogenesis.

METHODS: Intestine and colon from mice expressing a CTE-associated mutant form of EpCAM (mutant mice) were evaluated for specific markers by quantitative real-time polymerase chain reaction, Western blotting, and immunostaining. Body weight, blood glucose, and intestinal enzyme activity were also investigated. Enteroids derived from mutant mice were used to assess whether the decreased census of major secretory cells could be rescued.

RESULTS: Mutant mice exhibited alterations in brush-border ultrastructure, function, disaccharidase activity, and glucose

absorption, potentially contributing to nutrient malabsorption and impaired weight gain. Altered cell differentiation in mutant mice led to decreased enteroendocrine cells and increased numbers of nonsecretory cells, though the hypertrophied absorptive enterocytes lacked key features, causing brush border malfunction. Further, treatment with the Notch signaling inhibitor, DAPT, increased the numbers of major secretory cell types in mutant enteroids (graphical abstract 1).

CONCLUSIONS: Alterations in intestinal epithelial cell differentiation in mutant mice favor an increase in absorptive cells at the expense of major secretory cells. Although the proportion of absorptive enterocytes is increased, they lack key functional properties. We conclude that these effects underlie pathogenic features of CTE such as malabsorption and diarrhea, and ultimately the failure to thrive seen in patients. *(Cell Mol Gastroenterol Hepatol 2021;12:1353–1371; https://doi.org/10.1016/j.jcmgh.2021.06.015)*

Congenital tufting enteropathy (CTE) (Online Mendelian Inheritance in Man: 613217) is a rare intractable diarrheal disease of infancy characterized by profuse watery diarrhea, electrolyte imbalances, and

impaired growth.[1,2] Its intestinal pathology includes villous atrophy, crypt hyperplasia, and epithelial tufts leading to intestinal failure. CTE belongs to a family of congenital diarrhea and enteropathies that are both secretory and osmotic in nature.[1] Mutations in epithelial cell adhesion molecule (EpCAM) were identified as the primary cause for CTE.[3] Although serine peptidase inhibitor Kunitz type 2 (SPINT2) mutations have also been reported in a syndromic form of the disease, most CTE patients possess mutations in EpCAM.[4] Patients with CTE typically depend on parenteral nutrition and rarely achieve enteral autonomy without intestinal transplant. The significant morbidity and mortality associated with the disease suggest an urgent need for an improved understanding of disease pathophysiology, with the hope of contributing to the development of therapeutics.

Studies utilizing various in vivo, ex vivo, and in vitro generated models of CTE with EpCAM mutations have revealed some insights regarding the onset of the disease phenotype. EpCAM knockout mice have dysregulated E-cadherin and β-catenin in the enteric mucosa, leading to crypt-villus disorganization.[5] A study using a neonatal murine model bearing an EpCAM mutation identified in a CTE patient showed neonatal lethality, growth retardation with epithelial tufts, enterocyte crowding, altered desmosomes, and intercellular gaps similar to human CTE patients.[6] Another study of adult mice bearing the same mutation revealed growth retardation, CTE-like histopathology, impaired intestinal barrier function and decreases in the tight junction proteins zonula occludens-1 (ZO-1) and occludin.[7] CTE intestinal organoids from mice reveal alterations in differentiation in addition to barrier dysfunction.[8] Moreover, data suggest that deficiency of EpCAM in a colonic cell line is accompanied by ion transport and barrier defects.[7] These barrier defects may contribute to the secretory portion of CTE-associated diarrhea.[9–11] Further, while CTE patients have features of nutrient malabsorption, the role epithelial dysfunction plays in this aspect of the disease has yet to be understood.

The fact that most mice with engineered mutations in EpCAM exhibited intestinal failure suggests an important role for EpCAM in maintaining intestinal epithelial organization.[5,6,11,12] However, there is still much to be elucidated about the mechanistic role of mutant EpCAM in intestinal cellular organization. Via a tightly regulated program of differentiation, stem cells give rise to intestinal epithelial cells (IECs) that can be categorized as either absorptive cells or as 4 different secretory cell lineages: goblet, Paneth, enteroendocrine, and tuft cells. Intestinal stem cells (ISCs) continuously self-renew to generate an intermediate cell type, known as transit amplifying cells, which then undergo terminal differentiation and maturation to absorptive and secretory IECs to maintain intestinal cellular homeostasis.[13] The NOTCH and ATOH1 (MATH1) pathways play a crucial role in intestinal function by regulating the choice between absorptive and secretory lineages.[14–17] Previous studies in CTE patients as well as in mice engineered to express mutant EpCAM and enteroids derived therefrom revealed decreases in Paneth and goblet cell numbers,[8] which may indicate an alteration in IEC

differentiation. Thus, detailed investigation of the IEC differentiation pathway and its contributions to CTE pathogenesis was of interest.

Recent studies have also revealed a role for defective absorptive enterocytes in the pathogenesis of various intestinal conditions including congenital diarrheal disorders[18] such as congenital lactase deficiency,[19] glucose-galactose malabsorption,[20] sucrase-isomaltase deficiency,[21] congenital chloride diarrhea,[22] and microvillous inclusion disease (MVID).[23,24] Broadly, these diseases are accompanied by deficits in brush border-associated enzymes and transporters, as well as defects in intracellular protein transport, intracellular lipid transport, and intestinal barrier function.[25] Past studies utilizing different CTE models primarily focused on intestinal barrier function disruption and tight junction disorganization. However, the impact of loss of EpCAM on absorptive enterocyte maturation or function has not been studied. We reasoned that a deeper knowledge of the differentiation of absorptive enterocytes would broaden our understanding of CTE pathobiology.

In the present study, we hypothesized that a loss-of-function mutation of EpCAM results in an altered lineage differentiation cascade and defective absorptive enterocytes that contribute to CTE pathogenesis. Hence, the IEC differentiation cascade and functional markers of mature absorptive enterocytes were systematically evaluated.

Results

Mice With Inducible Expression of Mutant EpCAM Exhibit Impaired Weight Gain Upon Disease Onset

To expand our knowledge of primary and ancillary pathological features due to mutation of EpCAM, our previously described adult mutant mice with inducible expression of mutant EpCAM were utilized (hereafter referred to as mutant mice).[7] While characteristic features of small intestinal histopathology and epithelial barrier properties of CTE had already been described in these mutant mice, failure to thrive or poor weight gain had not been evaluated, despite it being a predominant symptom of CTE.[7] We therefore monitored the growth of both control and mutant mice over the course of 5 days. While control mice exhibited steady weight gain, mutant mice were noted

to have impaired growth beginning on day 4 of the observation period (Figure 1A), similar to CTE patients and our previous study in neonatal mice.[6] In order to check whether the diseased mice have diarrhea similar to CTE patients, evaluation of water content in the fecal material was undertaken. Despite the lack of growth in the mutant mice, water content of the stool was comparable between control and mutant mice at each time point (days 1, 3, and 5) (Figure 1B).

Impaired Glucose Absorption and Lack of Digestive Enzyme Activity in Mutant Mice

The lack of weight gain in mutant mice led us to evaluate nutrient absorption in these animals. Nutrient malabsorption can be attributed to mechanisms such as lack of intraluminal carbohydrate breakdown due to loss of brush border hydrolases, as well as transporter defects. As CTE affects the intestinal epithelium that contributes to these physiological processes, we set out to investigate whether malabsorption was a consequence of loss of absorption or a lack of intestinal brush border hydrolases. Carbohydrates are a primary source of caloric intake, especially in children, and thus carbohydrate absorption was examined in the form of an oral glucose tolerance test. Glucose uptake was significantly blunted in mutant mice compared with control mice at 10, 30, and 90 minutes after glucose administration (Figure 1C).

To investigate whether brush border hydrolases are impacted in our mutant mouse model, enzymes exclusively synthesized by enterocytes in the small intestine were the primary focus. We measured mucosal activity of sucrase, maltase, and lactase in mutant and control mice. Activity of all 3 enzymes was significantly decreased in mutant mice compared with control mice (Figure 1D). Among the 3, lactase activity was most severely affected (average 8-fold). To study whether the decreased hydrolase activity simply reflects the altered intestinal epithelial structure in the mutant mice, we also measured activity of intestinal alkaline phosphatase. In contrast to the other digestive enzymes studied, intestinal alkaline phosphatase activity was elevated in mutant mice compared with control mice (Figure 1D). Overall, our data suggest that a significant and selective decrease in brush border digestive enzyme activity contributes to the malabsorption seen in CTE.

Mutant Mice Have Decreased Numbers Of Chromogranin A–Expressing Enteroendocrine Cells and Increased Numbers of Nonsecretory Epithelial Cells

A significant decrease in Paneth and goblet cell numbers in CTE patients and corresponding mutant mice has previously been reported.[8] In order to assess whether other major secretory cell types are affected in CTE, we evaluated numbers of enteroendocrine cells in the mutant mice. Staining for the specific enteroendocrine cell marker, chromogranin A (CHGA) revealed a decrease in the percentage of enteroendocrine cells in mutant mice compared with control mice (Figure 1E). This result confirms that CHGA-positive enteroendocrine cells are likely affected in CTE along with Paneth and goblet cells. We also examined epithelial cells of the absorptive lineage in the mutant mice by counting nonsecretory epithelial cells in the intestinal epithelium. Despite evidence for decreased epithelial absorption in the mutant mice, the number of nonsecretory epithelial cells was significantly increased in mutant mice compared with control mice (Figure 1D). This is also consistent with our finding of increased alkaline phosphatase activity.

Evaluation of Gene Expression Characteristics of IEC Types

The apparent reciprocal alteration in secretory and nonsecretory intestinal cell types in mutant mice led us to further investigate cell differentiation at the molecular level. Because mutant mice have decreased enteroendocrine cells compared with control mice, CHGA was evaluated at the gene level. In line with the immunohistochemistry (IHC) findings (Figure 1D), messenger RNA (mRNA) expression for CHGA was decreased in mutant mice compared with control mice (Figure 2A). In order to further understand the dynamics of IEC differentiation in mutant mice, markers that define ISCs, progenitor cells, transit amplifying cells, and enterocyte differentiation markers were chosen. The classical long-lived, self-renewing multipotent ISCs were assessed by studying expression of leucine-rich repeat-containing G protein–coupled receptor 5 (LGR5) and BMI1 proto-oncogene, polycomb ring finger (BMI1).[26] There was a significant decrease in expression of LGR5, a marker of mitotically active ISCs, in mutant mice compared with control mice (Figure 2A). On the contrary, expression of BMI1, a marker of quiescent ISCs, was not changed between CTE mutants and control mice. Similarly, there was no difference in mRNA levels for the ISC regulator achaete-scute family BHLH transcription factor 2 (ASCL2),[27] the robust surrogate stem cell marker olfactomedin-4 (OLFM4),[28] or the early lineage/transit amplifying progenitor/stem cell markers prominin 1 (PROM1),[29] Musashi RNA binding protein 1 (MSI1),[30] and intestinal epithelial differentiation homeobox transcription factor caudal type homeobox 2 (CDX2)[31] between control and mutant mice (Figure 2A). These results indicate that there is decreased mRNA expression for markers of some cell types (enteroendocrine cells and ISCs) in mutant mice while markers for other stem or progenitor cells and differentiation markers are unchanged, indicating no direct role of EpCAM in those cell types.

Mutant Mice Show Alterations in ISC Differentiation Cascades

Our previous and current findings of a decreased number of goblet cells, Paneth cells, and enteroendocrine cells along with decreased gene expression of CHGA and LGR5 in mutant mice led us to study signaling molecules and transcription factors that regulate the secretory pathway and their role in IEC differentiation. ATOH1 has been shown to be essential for secretory cell differentiation both in the
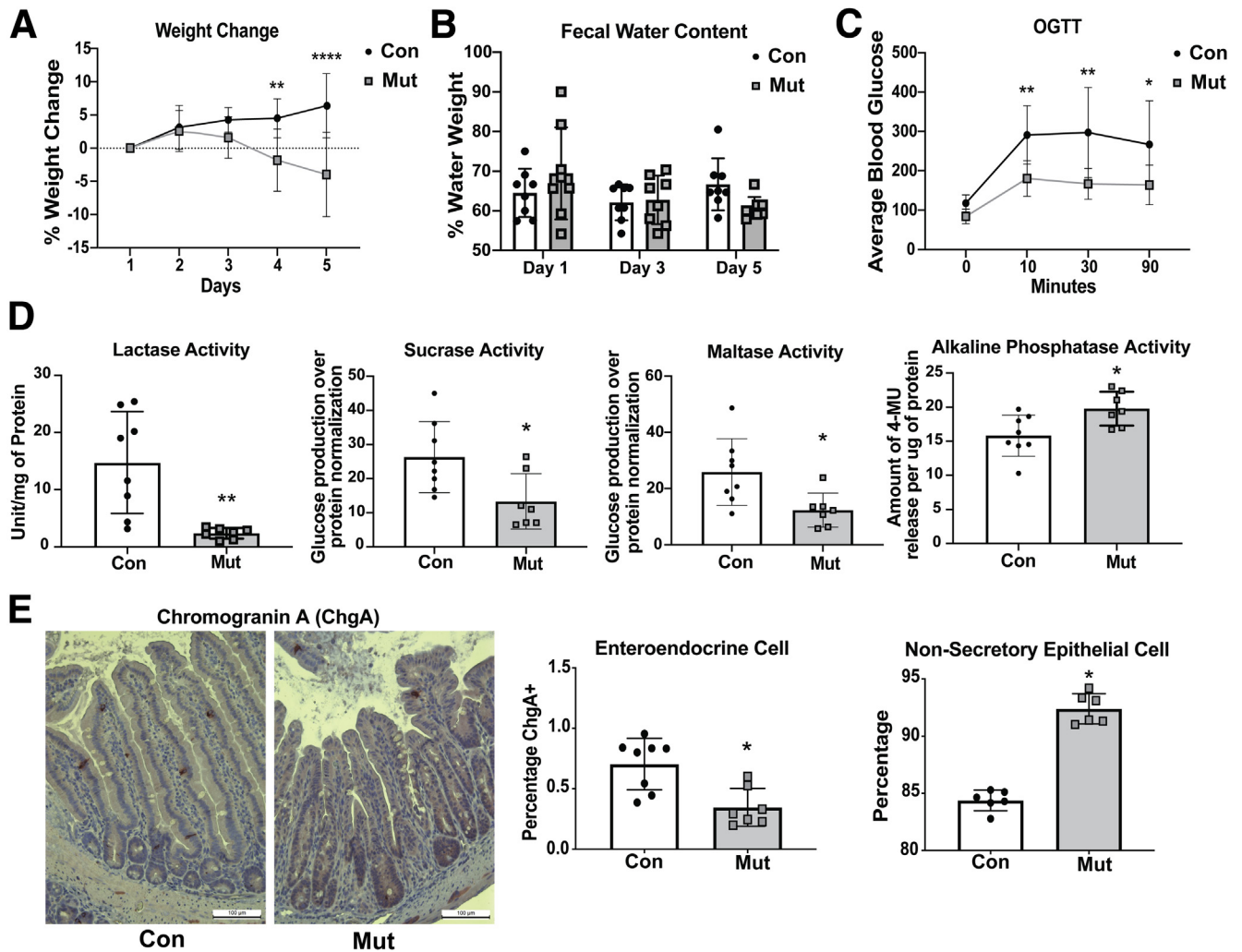
Figure 1. Pathologic features of mutant mice. (A) Percentage weight change from day 1 in mutant mice (Mut) and control mice (Con) over 5 days with weight loss in Mut compared with Con mice (n = 8). Tamoxifen was administered on days 1 and 2 to induce expression of mutant EpCAM. (B) Percentage of stool water content in Con and Mut mice (n = 8) on days 1, 3, and 5. Unchanged water weight percentage between Con and Mut mice. (C) Oral glucose tolerance test (OGTT) at day 5. Decreased blood glucose levels in Mut compared with Con mice at 10, 30, and 90 minutes (n = 5). (D) Decrease in lactase, sucrase, and maltase activity and increased alkaline phosphatase activity in duodenal lysate of Mut mice (n = 7) compared with Con mice (n = 8) at day 5 of treatment. (E) Representative IHC bright-field (20×) images showing decreased percentage of ChgA⁺ cells (enteroendocrine cells) in Mut mice (n = 7) compared with Con mice (n = 8) and increased number of nonsecretory epithelial cells relative to total epithelial cells (n = 6). Scale bar = 100 μm. *$P < .05$, **$P < .01$, ***$P < .001$, ****$P < .0001$ by Student's t test in all results.

adult intestine and in the embryo.[13] Thus, cells expressing ATOH1 are driven toward a secretory cell lineage (Paneth, enteroendocrine, goblet) compared with those driven by NOTCH, which instead follow an absorptive path.[32,33] A significant decrease in mRNA for *ATOH1* in mutant mice corresponded with the observed decrease in major secretory IEC lineages (Figure 2B). This was further confirmed by detecting decreased ATOH1 protein in these mice (Figure 2C). Unlike *ATOH1*, the gene expression of another intestinal secretory lineage transcription factor, *Hnf1α*, was not significantly changed in mutant mice compared with control mice (Figure 2B). ATOH1 downstream signaling was also evaluated at the mRNA level, where we observed a significant decrease in Krüppel-like factor 4 (*KLF4*)

expression in mutant mice while the expression of neurogenin 3 (*NEUG3*) and *SOX9* were unchanged compared with control mice. We also evaluated factors that promote absorptive lineage differentiation. Although there were no changes in expression of mRNA for *NOTCH1* (Figure 2B) and its downstream transcription factor *HES1* in mutant mice (Figure 2B and C), increased protein expression of Notch intracellular domain (NICD) by immunofluorescence (the active signal transducer of absorptive lineage specification) (Figure 2D) corresponded with a bias toward nonsecretory cell differentiation. In summary, cell differentiation signaling studies in mutant mice indicate a bias toward absorptive and away from secretory lineage IEC differentiation. This is consistent with the increased number of nonsecretory
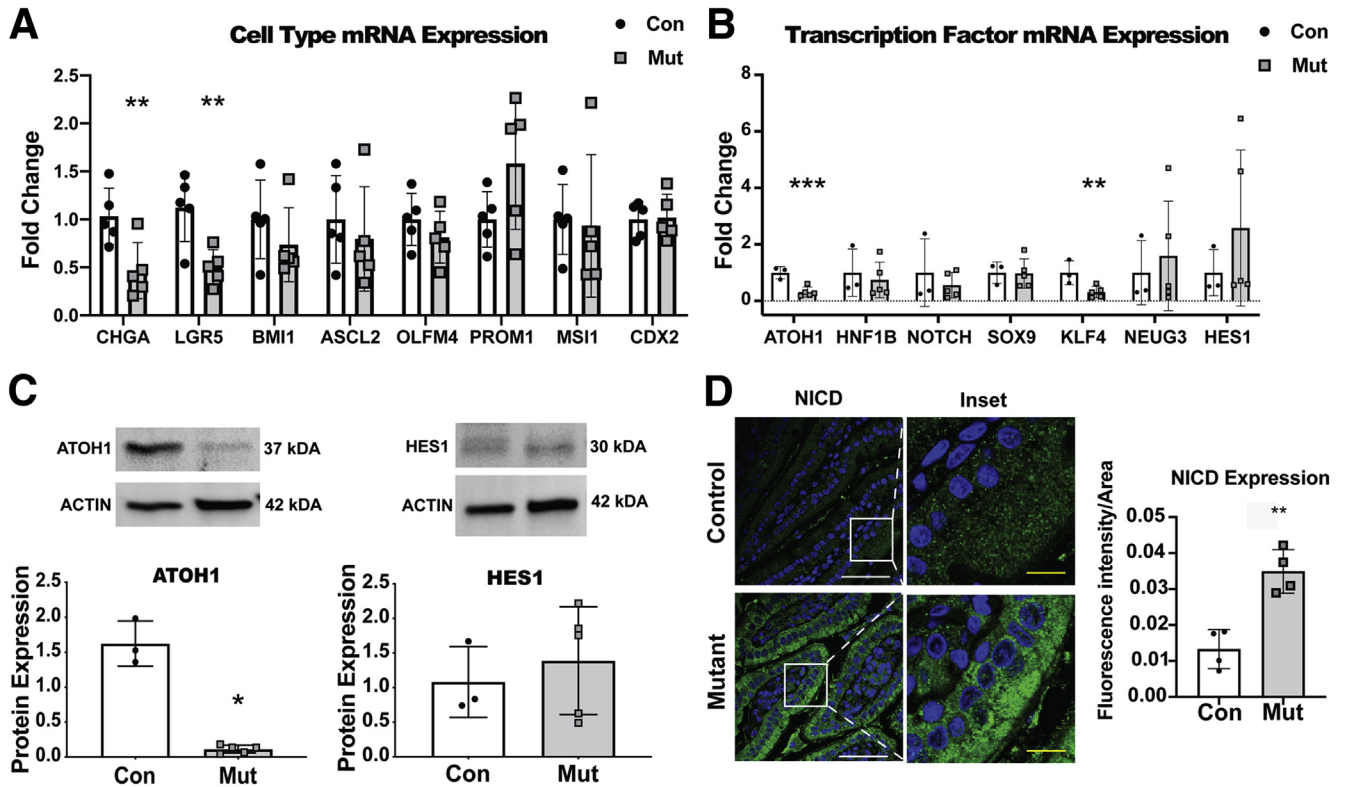
Figure 2. IEC differentiation in mutant mice. (*A*) Cell-type mRNA expression. Decreased expression of CHGA (enteroendocrine cell) and LGR5, with normal levels of progenitor and transient amplifying cell markers *BMI1*, *ASCL2*, *OLFM4*, *PROM1*, *MSI1*, and *CDX2* in small intestinal tissue lysates from mutant (Mut) mice compared with control (Con) mice (n = 5). (*B*) mRNA expression of transcription factors. Decreased expression of *ATOH1* and *KLF4* with stable expression of *HNF1b*, *NOTCH*, *SOX9*, *NEUG3*, and *HES1* in small intestinal tissue lysates of Mut mice compared with Con mice (n = 5). (*C*) Representative Western blot images for ATOH1 and HES1, relative to actin in small intestinal tissue lysates from Con and Mut mice (n = 5). Decreased protein expression of ATOH1 with unchanged expression of HES1 in Mut mice compared with Con mice. (*D*) Representative immunofluorescent images of intestinal tissue section showing NICD staining (green) and nucleus (blue) in Con and Mut mice. The bar graph shows the increased NICD fluorescent intensity expression per area in the Mut mice when compared with the Con mice (n = 4). White scale bar = 50 μm. Yellow scale bar = 10 μm. *$P < .05$, **$P < .01$, ***$P < .001$, ****$P < .0001$ by Student's *t* test for all results.

epithelial cells and decreased goblet cells, Paneth cells and enteroendocrine cells in mutant mice as described[8] and expanded here (Figure 1D). The current study also accords with our previous work in mutant enteroids that showed reduced major secretory cell differentiation.[8]

Enterocytes Lack Expression of Key Functional Markers

Although our cell differentiation results suggested an increase in nonsecretory lineage cells in mutant mice, the pathological features seen in CTE patients indicate defective absorption. The secretory nature of diarrhea in CTE patients led us to study ion transporters characteristic of absorptive enterocytes. Moreover, our findings of malabsorption and lack of brush border enzymes responsible for carbohydrate digestion in mutant mice also suggested malfunction of absorptive enterocytes despite an increase in their number. We hypothesized that although enterocytes are increased in number in mutant mice, they are not fully functional due to a lack of key proteins, perhaps secondary to their hypertrophy. Hence, additional molecular and functional markers

of typical absorptive enterocytes were assessed in the mutant mice. mRNA studies for apical markers showed a decrease in the ion transporter downregulated in adenoma (*DRA*) and the water channel aquaporin 7 (*AQP7*) in mutant mice, while mRNA for another apical transporter, sodium-hydrogen exchanger 3 (*NHE3*) and the enterocyte structural marker, villin, were unchanged compared with control mice (Figure 3A). Evaluating basolateral transporters, we found a significant reduction in mRNA levels for anion exchanger 2 (*AE2*) and both alpha and beta subunits of Na, K, ATPase (*ATPA1*, *ATPB1*) in mutant mice while the expression of sodium bicarbonate cotransporter 1 (*NBC1*) was unchanged compared with control mice (Figure 3B). These data suggest altered expression of some, but not all, ion transporters in mutant EpCAM enterocytes, and could explain defective water and electrolyte absorption in this disease. The decreased ability of mutant mice to absorb glucose, as shown by the oral glucose tolerance test results, also led us to examine expression of glucose transporters in the small intestine. mRNA levels for sodium-glucose transporter 1 (*SGLT1*) and glucose transporter 2 (*GLUT2*), which are responsible for the majority of glucose transport from
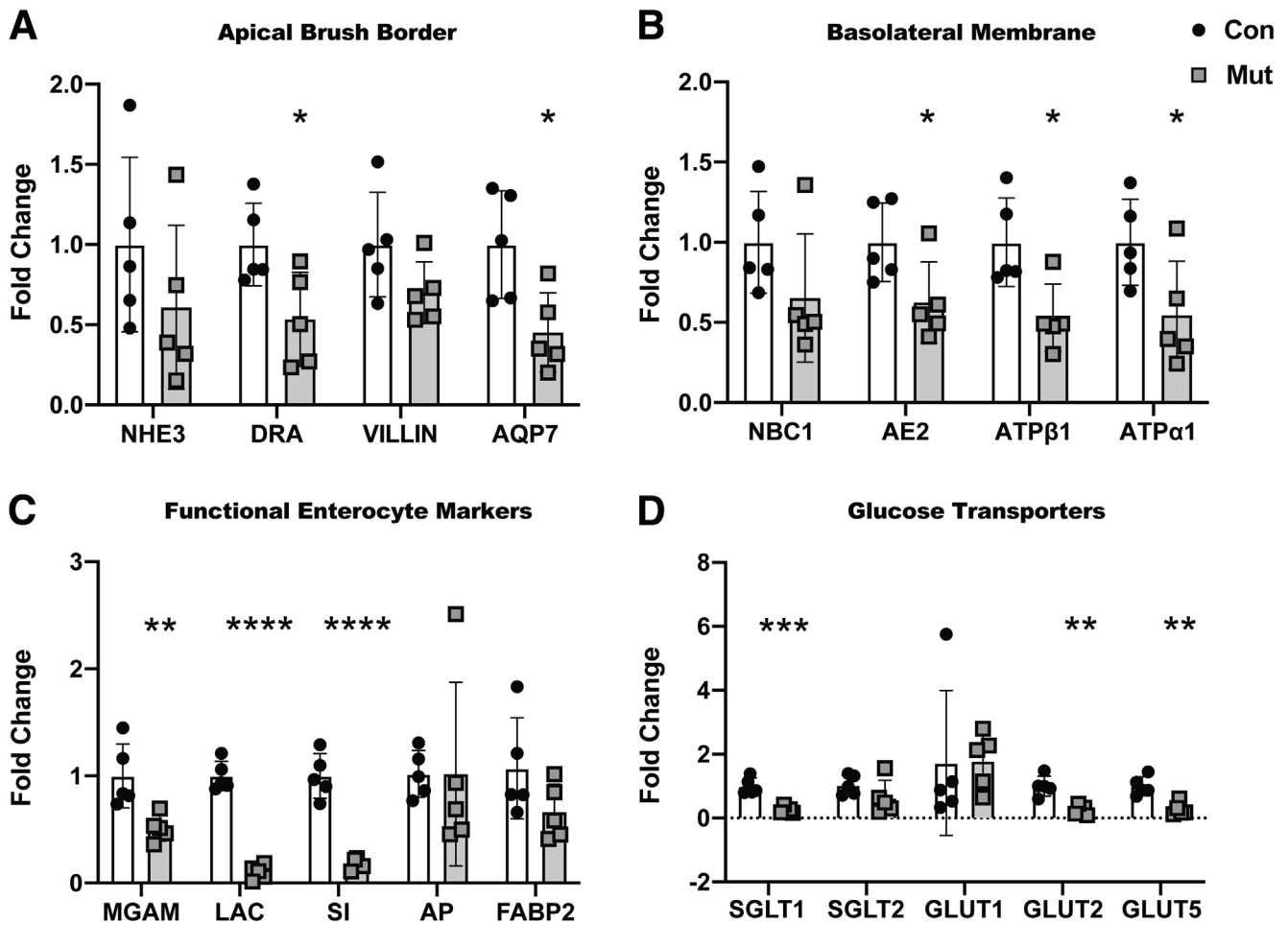
Figure 3. Functional enterocyte gene markers in mutant mice. (*A*) Decreased mRNA expression for apical brush border markers downregulated in adenoma (*DRA*) and aquaporin 7 (*AQP7*) with normal levels of sodium hydrogen exchanger 3 (*NHE3*) *and VILLIN* in intestinal tissue lysates of mutant (Mut) mice compared with control (Con) mice (n = 5). (*B*) Decreased mRNA expression for basolateral anion exchanger 2 (*AE2*), ATPase beta 1 (*ATPβ1*), and ATPase alpha 1 (*ATPα1*) in intestinal tissue lysates of Mut mice when compared with Con mice (n = 5) with normal levels of membrane marker sodium bicarbonate cotransporter 1 (*NBC1*). (*C*) Decreased mRNA expression for functional enterocyte markers maltase glucoamylase (*MGAM*), lactase (*LAC*), and sucrase isomaltase (*SI*) with normal expression of alkaline phosphatase (*AP*) and fatty acid binding protein 2 (*FABP2*) in intestinal tissue lysates in Mut mice compared with Con mice (n = 5). (*D*) Decreased mRNA expression of glucose transporters sodium-glucose cotransporter 1 (*SGLT1*) and glucose transporters 2 and 5 (*GLUT2*, *GLUT5*) and normal expression of *SGLT2* and *GLUT1* in intestinal tissue lysates in Mut compared with Con mice (n = 5). *$P < .05$, **$P < .01$, ***$P < .001$, ****$P < .0001$ by Student's t test for all results.

the small intestinal lumen to blood, were significantly decreased in mutant murine intestine compared with control mice. Additionally, expression of *GLUT5*, a major fructose transporter of the small intestine, was also significantly decreased in the mutant mice compared with control mice (Figure 3*D*). On the other hand, the lack of change in mRNA expression for *SGLT2* and *GLUT1* as well as for villin between the 2 groups of mice implied the presence of equivalent brush border membranes between the groups. Altered expression of glucose transporters might explain the compromised glucose absorption seen in mutant mice. Decreased disaccharidase activity in mutant mice also prompted investigation of expression of enterocyte-specific genes that aid in digestion and maintaining physiological homeostasis. Expression of enzymes involved in carbohydrate digestion, including maltase-glucoamylase (*MGAM*),

lactase (*LAC*), and sucrase-isomaltase (*SI*), was found to be significantly decreased in mutant mice compared with control mice (Figure 3*C*). On the other hand, expression of other villous epithelial markers, such as intestinal alkaline phosphatase (*Alk-Phos*) and fatty acid binding protein 2 (*Fabp2*) was equivalent between the 2 groups. These gene expression results support the findings of selectively decreased disaccharidase activity in mutant mice. Therefore, enterocytes in CTE lack key functional markers, which may contribute to disease pathology.

Owing to evidence for altered gene expression of various apical and basolateral membrane markers, including glucose transporters, in mutant mice, protein expression was evaluated by Western blot. The structural protein, villin, and the ion transporter, DRA, were present at comparable levels in both control and mutant mice. Protein expression for villin is in line

with its mRNA expression, confirming that the expression of villin is unchanged between control and mutant mice. Although the mRNA expression of DRA is decreased between control and mutant mice, protein expression was found to be equivalent between the groups. This may imply that DRA protein levels are relatively stable, and thus less subject to alteration than mRNA. As both RNA and protein studies were performed at a single time point, it is possible that the decrease of DRA mRNA has yet to result in downregulated DRA protein expression. Importantly, protein levels of NHE3 and SGLT1 were significantly decreased in mutant mice compared with control mice (Figure 4A). These results further confirm the deficiency of key markers in mutant enterocytes.

The decrease in gene and protein expression and disruption in the function of absorptive enterocytes led us to question the location of enterocyte membrane proteins in the intestinal epithelium. In order to test this, immunofluorescent and IHC staining was performed for NHE3, villin, and SGLT1 on small intestinal sections from control and mutant mice. No changes were found in the expression and localization of villin between the groups, confirming an intact brush border. Conversely, staining of SGLT1 and NHE3 was abberant in mutant mice (Figure 4B). Both markers lacked uniform staining along the brush border membrane in mutant mice, whereas uniform expression of these markers was noted throughout the brush border membrane in control mice.

Mutant Mice Show Defects in Brush Border Ultra-Structure

As some key enterocytes brush border markers were altered in the mutant mice while other markers were unchanged, we evaluated brush border ultrastructure on the apical surface of the enterocytes. Ultrastructural analysis was performed on electron micrographs to evaluate the length and packing of microvilli. Electron micrographs revealed variability and an overall reduction in the length of microvilli in mutant intestinal tissue sections while control mice showed uniformity (Figure 4C). On the other hand, no significant changes were found in microvillus packing density between control and mutant mice (Figure 4C). The unchanged microvilli packing density suggests no significant changes in microvillus number between control and mutant mice. Nevertheless, the ultrastructural changes in the brush border of the mutant mice further confirm brush-border defects.

Notch Pathway Inhibition Increased Major Secretory Cell Markers in Mutant Enteroids

Our findings of aberrant epithelial differentiation in mutant mice, resulting in an increase in the absorptive lineage and decreased major secretory lineage cells as well as the identification of potentially affected signaling pathways led us to investigate whether these discrepancies could be rescued by targeting relevant signaling pathways. Because Notch intercellular domain was increased in epithelial cells of mutant mice (Figure 2C), Notch signaling was targeted. Notch pathway signaling was inhibited with

the γ-secretase inhibitor, DAPT, in mutant enteroid-derived monolayers (EDMs). In order to confirm that EpCAM was mutated in mutant EDM, quantitative real-time polymerase chain reaction (qRT-PCR) was performed for the mutated region (EPCAM exon 3–4) compared with an untargeted region (EPCAM exons 6–7). Significantly decreased expression of EPCAM exons 3–4 to exons 6–7 mRNA was observed in the mutant EDM or mutant EDM additionally treated with DAPT after 48 hours of treatment with TAM compared with their respective control EDMs (Figure 5A), confirming the mutation of EpCAM in the mutant EDM groups.

In order to confirm whether DAPT inhibited the Notch signaling pathway and promoted the secretory cell differentiation, control EDMs were treated with DAPT and compared with untreated control EDMs. mRNA expression for the Paneth cell marker, lysozyme, the goblet cell marker, mucin 2, and the enteroendocrine cell marker, CHGA, was found to be upregulated in DAPT-treated control EDMs when compared with untreated EDMs (Figure 5B). The downregulation of Notch1 mRNA and its downstream signaling transcription factor Hes1 in DAPT-treated EDM further confirms DAPT as a potent inhibitor of the Notch signaling pathway and a promotor of secretory lineage differentiation. Although there were no significant differences in expression of mRNA for the transcription factor ATOH1, NEUG3, another secretory lineage transcription factor, was upregulated in control EDM treated with DAPT (Figure 5B). Considering effects of DAPT treatment in mutant EDM, we investigated whether DAPT could rescue the decrease in Paneth, goblet and enteroendocrine cells in mutant EDM. Indeed, DAPT increased mRNA for lysozyme, mucin 2, and CHGA compared with mutant enteroids without any treatment (Figure 5C). Expression of mRNA for transcription factors relevant to the secretory and absorptive pathways was also examined. ATOH1 and NEUG3 were increased in DAPT-treated mutant enteroids compared with untreated mutant enteroids, while NOTCH1 and HES1 expression was not affected. Though speculative, the drive toward Notch signaling that is induced by EpCAM mutation may render the mutant cells less sensitive to DAPT. These results suggest that aberrant Notch signaling may be targeted to improve the balance of cell differentiation in a model of CTE.

To confirm these results, markers of major secretory cells were evaluated at the protein level. In line with the mRNA findings, DAPT increased the number of secretory cells in mutant EDMs. Thus, the proportions of lysozyme-positive (Paneth cells), PAS-positive (goblet cells) and CHGA-positive (enteroendoocrine) cells were significantly increased in DAPT-treated mutant EDMs compared with untreated mutant EDMs (Figure 5D). This result may suggest a potential therapeutic target to restore decreased Paneth cells, goblet cells, and enteroendocrine cells in CTE disease.

CTE-Associated Changes in Epithelial Homeostasis Primarily Affected the Small Intestine

Although CTE manifests primarily in the small intestine of human patients and results in severe intestinal failure,[2]

the colonic mucosa has also been reported to be involved.[1] We therefore examined whether EpCAM mutation impacts epithelial biology in 2 other gastrointestinal epithelial organs, the colon and pancreas. To evaluate the effect of mutant EPCAM in the colon, hematoxylin and eosin (H&E)

staining as well as qRT-PCR of glucose transporters and markers of the apical brush border were performed. H&E staining revealed that the overall architecture of the colon was preserved in mutant mice compared with control mice. The colonic epithelium displayed mild cellular
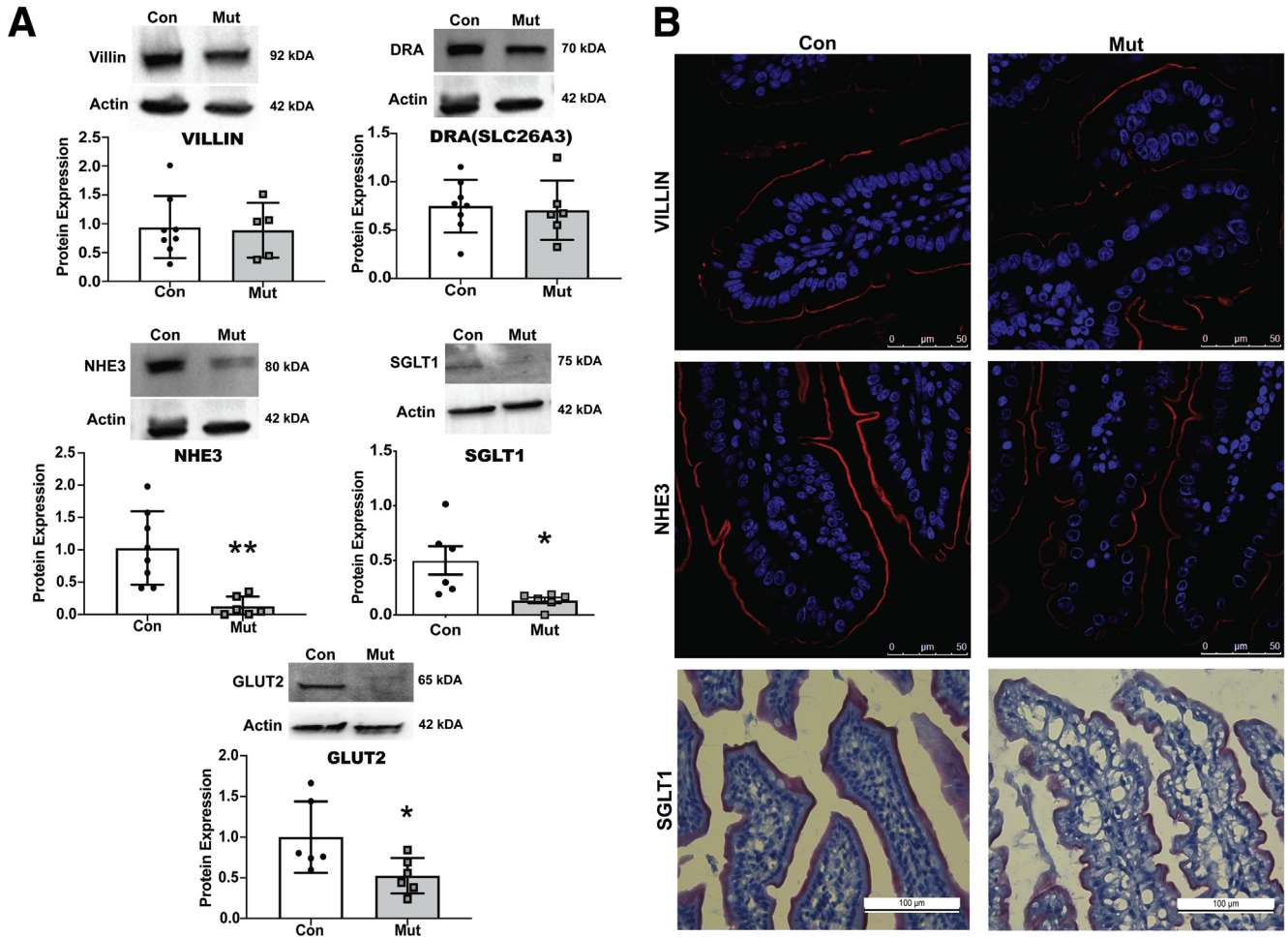
disorganization along the brush border in mutant mice compared with control mice (Figure 6A). No change was found in mRNA expression for any of the glucose transporters markers (*SGLT1, SGLT2, GLUT1, GLUT2*, and *GLUT5*), apical membrane makers (*Villin, AQP7, DRA, NHE3*, alpha and beta subunit of epithelial sodium channel) and basolateral membrane markers (*ATPα1, ATPβ1, NBC1*, and *AE2*) in colonic tissue studied between control and mutant mice (Figure 6B and C). In the pancreas, H&E staining revealed no change in acinar cells, islets of Langerhans, or interlobular ducts between control and mutant mice (Figure 7A). Finally, to further investigate whether EpCAM mutants influence pancreatic activity, serum lipase and amylase were evaluated in control and mutant mice. Equivalent serum lipase and amylase activity in control and mutant mice (Figure 7B) suggests that pancreatic function is likely to be normal in mutant mice. These experiments confirm that CTE most severely targets the small intestine.
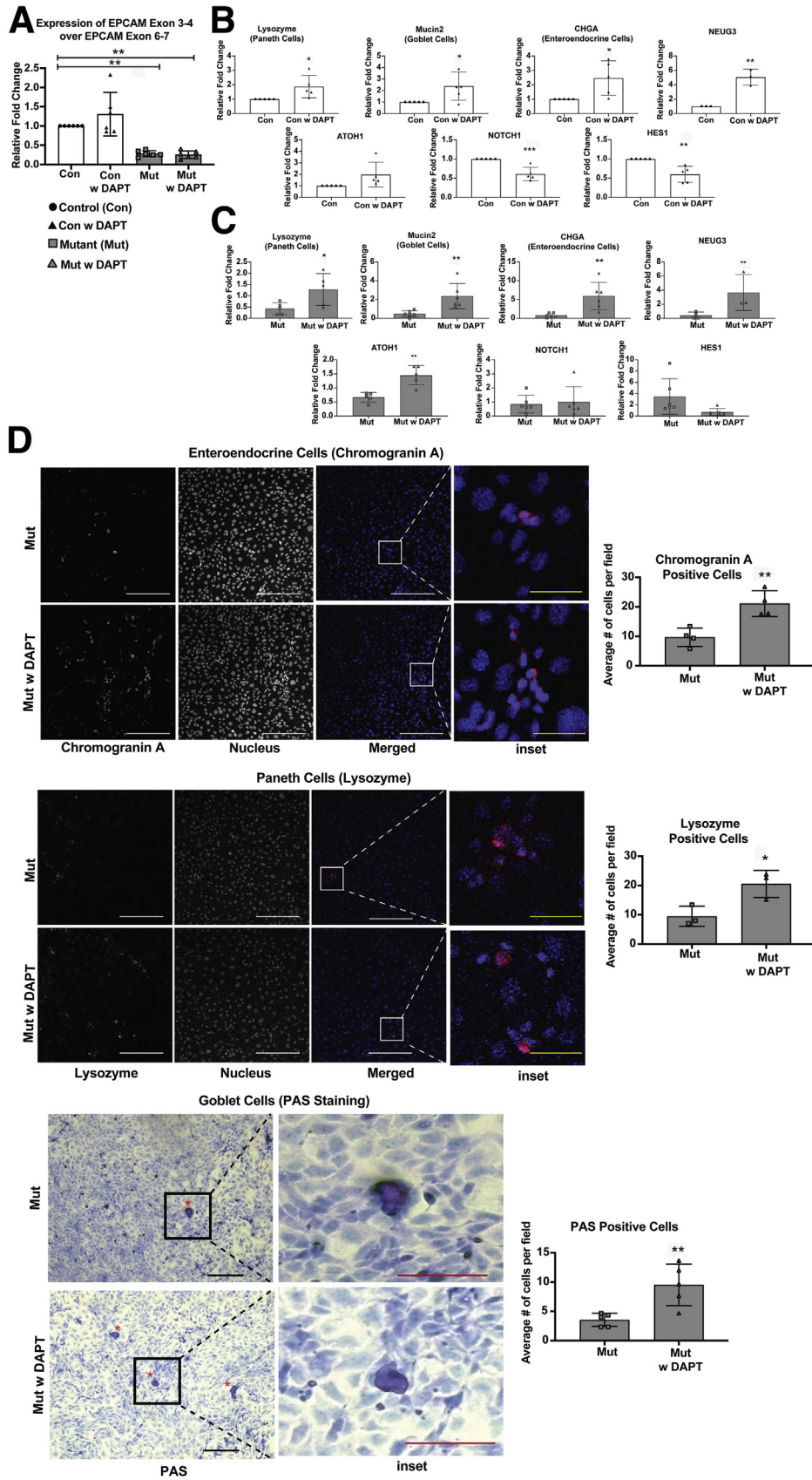
Discussion

Previously, studies in mutant EpCAM murine models have revealed alterations in histopathology, epithelial barrier, and ion transport function, and decreased major secretory cells that contribute to CTE pathology.[6,7] Studies have also suggested decreased major secretory epithelial cells in different CTE models (patient, mice, enteroids),[8] though alterations in the differentiation cascade that lead to differentially expressed cell types had not been investigated. Moreover, despite knowledge of the classical pathological features in CTE, their relationship to the nutrient malabsorption observed in patients[1] had not been studied in any CTE model. The biology behind the signs and symptoms in CTE patients, such as impaired growth and the secretory, as well as osmotic nature of diarrhea, remained elusive. The current study shows that a murine model of CTE, bearing a mutation in EpCAM, exhibits alterations in small intestinal epithelial diffentiation. The aberrant lineage differentiation cascade in CTE mice leads to decrease of major secretory cells and increased nonsecretory epithelial cells. Moreover, treatment of our enteroid model with the γ-secretase inhibitor, DAPT, provides a therapeutic suggestion to rescue faulty lineage differentiation. Our study also suggests that despite their increased numbers, absorptive enterocytes are dysfunctional and likely are major

contributors to pathology characteristic of CTE, such as malabsorption, reduced caloric uptake, secretory and osmotic diarrhea, and weight loss.

Failure to thrive, impaired growth, and diarrhea are hallmarks of CTE.[1] A lack of weight gain has been reported in constitutive CTE neonatal mice.[6] In the current study, weight loss also validates the adult model system. Although adult mutant mice previously demonstrated increased barrier permeability,[7] here we found no significant increase in fecal water content in mutant mice when compared with the control mice. As the water intake of the mice was not rigorously monitored, it may differ between control mice and mutants, confounding the results. This could also be related to our finding that the colon is spared in this model, and thus could salvage excess fluid originating from the diseased small intestine. Moreover, murine models typically are less likely to exhibit frank diarrhea compared with humans with similar physiology. Failure to thrive and weight loss also suggest undernutrition due to inadequate caloric intake, absorption, or excessive energy expenditure. The growth failure in mutant mice provided an impetus for an evaluation of malabsorption. The clinical observation that enteral feeding often worsens the symptoms of CTE with parenteral nutrition being the most reliable source of nutrients in these patients also indicates the involvement of malabsorption in the disease.[1] Because impaired growth worsens disease outcome because it leads to complications, treatments that alleviate weight loss may improve prognosis.

Lack of glycoside hydrolases (maltase, sucrase, and lactase) in the small intestinal brush border in CTE mice might lead to reduced digestion and availability of glucose for absorption, resulting in malabsorption of ingested calories. Because CTE appears in the neonatal period when milk is the major source of nutrient intake, a significant decrease in lactase activity in our mutant mice is consistent with impaired growth in CTE patients and models of the disease.[1,34,35] Moreover, both the lack of digestive enzyme activity and glucose malabsorption likely contribute to the osmotic diarrhea reported in CTE patients.[36] Although beyond the scope of this study, evaluation of additional hydrolases synthesized and secreted by the pancreas into the luminal content would provide further evidence as to whether brush border enzymes are selectively affected in CTE. Nevertheless, because pancreatic structure and

Figure 4. (*See previous page*). **Functional enterocyte markers at protein level in mutant mice.** (*A*) Representative Western blot images and quantification of *VILLIN*, downregulated in adenoma (*DRA*), sodium-hydrogen exchanger 3 (*NHE3*), sodium-glucose cotransporter 1 (*SGLT1*), and glucose transporter 2 (*GLUT2*) with respect to β-actin (*Actin*) in intestinal tissue lysates from control (Con) and mutant (Mut) mice, with decreased *NHE3*, *SGLT1*, and *GLUT2* expression and unchanged *VILLIN* and *DRA* expression. The same blot was used to detect DRA and *NHE3* protein. (*B*) Representative images of immunofluorescent staining of Con and Mut intestinal tissue section showing expression of *VILLIN* (Red) and Draq5 staining for nuclear DNA (blue) (upper panel); expression of *NHE3* (red) and Draq5 staining for nuclear DNA (blue) (middle panel). Representative bright-field images of immunohistochemical staining of Con and Mut intestinal tissue sections showing expression of *SGLT1*. *NHE3* and *SGLT1* lack uniform distribution along the brush border membrane in Mut tissue when compared with Con tissue, while there was no change in localization of *VILLIN* expression along the membrane (n = 3). Scale bar for all immunofluorescence images = 50 μm. Scale bar for bright-field images = 100 μm. (*C*) Representative images of electron microscopy in neonatal Con and Mut small intestinal tissue showing brush border microvilli. Red scale bar = 1 μm. The graphs describe the average well oriented microvilli height and number of microvilli per unit length from n = 3 samples. *$P < .05$, **$P < .01$, ***$P < .001$, ****$P < .0001$ by Student's t test for all results.

A Expression of EPCAM Exon 3-4 over EPCAM Exon 6-7

- Control (Con)
- ▲ Con w DAPT
- ■ Mutant (Mut)
- △ Mut w DAPT

B
Lysozyme (Paneth Cells), Mucin2 (Goblet Cells), CHGA (Enteroendocrine Cells), NEUG3, ATOH1, NOTCH1, HES1

C
Lysozyme (Paneth Cells), Mucin2 (Goblet Cells), CHGA (Enteroendocrine Cells), NEUG3, ATOH1, NOTCH1, HES1

D

Enteroendocrine Cells (Chromogranin A)

Chromogranin A | Nucleus | Merged | inset

Chromogranin A Positive Cells

Paneth Cells (Lysozyme)

Lysozyme | Nucleus | Merged | inset

Lysozyme Positive Cells

Goblet Cells (PAS Staining)

PAS | inset

PAS Positive Cells

function are not affected in CTE, it is likely that pancreatic-secreted enzymes would be normal in mutant mice, consistent with our finding of normal levels of circulating lipase and amylase. On the other hand, the increase in the activity of alkaline phosphatase, a ubiquitous intestinal enzyme in the mutant mice is interesting, as it suggests that the intestinal epithelium is still largely intact despite a decrease in one of its major functions.

Enteroendocrine cells comprise the largest endocrine system in the body and regulate physiological and homeostatic functions of the digestive tract by secreting multiple peptide hormones.[37] Thus, a decrease in enteroendocrine cell number in mutant mice might disrupt sensing of luminal content and activation of vagal afferent fibers to control food intake.[38] A lack of intestinal enteroendocrine cells is not unique to CTE, and is also seen in congenital anendocrinosis.[39] As with CTE, patients with congenital anendocrinosis have severe nutrient malabsorption leading to diarrhea.

ATOH1 is the master regulator that directs progenitor cells to the secretory cell fate.[40] Hence, the novel finding of decreased ATOH1 stemming from EpCAM mutation likely accounts for the aberrant cell census found in CTE.[8] On the other hand, an increase in NICD in mutant mice confirms CTE is likely accompanied by a drive away from differentiation to a secretory cell fate and toward the absorptive lineage. Rescue of the decreased secretory cells with DAPT treatment further suggests involvement of the Notch pathway in CTE and also potentially opens an avenue toward a future option to treat the aspects of CTE that could result from decreased secretory cells, such as the loss of coordination of digestion and absorption by enteroendocrine cells. Further research to explore this option is needed to interrogate whether the homeostasis of intestinal cell types is maintained after the treatment. On the contrary, overexpression of goblet cells could be detrimental for intestinal tissue, as in organoids they have been shown to disrupt epithelial contacts and increase permeability.[41] Hence, the ideal target would be rescue of the decreased secretory cells without overexpression of any cell type.

The increased Notch signaling in adult mutant mice explains the increased number of nonsecretory epithelial cells and upregulated alkaline phosphatase activity found in these mice. Of note, an increase in epithelial proliferation was reported in the neonatal CTE model.[6] The increased number of nonsecretory epithelial cells in adult mutant mice along with unchanged expression of Cdx2 and several other epithelial markers not only excludes a general detrimental effect of CTE on all IEC types, but also strongly supports an alteration in the IEC differentiation cascade. Because EpCAM is involved in pluripotency and maintenance of ISCs, the decreased expression of Lgr5 in mutant mice is probably due to a direct effect of EpCAM mutation. Endoplasmic reticulum stress is also reported to be responsible for loss of intestinal epithelial stemness[42] through activation of the unfolded protein response (UPR). Our prior finding of endoplasmic reticulum stress and UPR in CTE mice[43] may be the cause of the loss of Lgr5-positive ISCs in these mice. Further studies are needed to explain the direct mechanism by which mutant EpCAM affects Lgr5-positive ISCs but not other stem cells, transit amplifying cells, or other progenitor cells.

Our findings suggest some key markers of mature absorptive enterocytes are inappropriately reduced in mutant mice while expression of other markers is not changed. Decreased expression of key ion transporters, channel, or pumps at both basolateral and apical membranes may account for secretory diarrhea found in CTE patients. Reduced expression of SGLT1 and GLUT2 would lead to glucose malabsorption and less caloric intake in these mutant mice. Though it is beyond the scope of the current study to fully explain aberrant expression and localization of some but not all markers in affected enterocytes, we can speculate on some possible mechanisms. For example, EpCAM contributes to the formation of a functional apical junctional complex with adaptor molecules that play a role in regulating cell polarity.[44] Thus, the observation that NHE3 protein, but not mRNA, expression was reduced may imply post-transcriptional regulation via altered interactions with the PDZ domain protein, NHERF[45] that might impair the stability of NHE3. The ultrastructural

---

Figure 5. (*See previous page*). **Restoration of secretory epithelial lineages with Notch inhibition in mutant enteroids.** (*A*) mRNA expression of EPCAM exons 3–4 (mutated region) over EPCAM exons 6–7 (unchanged region) in EDM from control (Con), control EDM treated with DAPT (Con w DAPT), mutant EDM (Mut), and mutant EDM treated with DAPT (Mut w DAPT) group. Decreased expression of EPCAM exons 3–4 in the Mut and Mut w DAPT groups confirms induction of mutation in the respective group. (*B*) mRNA expression for cell-type markers (lysozyme, mucin 2, CHGA) and transcription factors (*ATOH1*, *HES1*, and *NOTCH*, neurogenin 3) in lysates from Control w DAPT or Con (n = 5 in all except neurogenin 3 where n = 3). The mRNA expression of lysozyme, mucin 2, CHGA, and neurogenin 3 were increased upon treatment with DAPT, while expression of *HES1* and *NOTCH* was decreased. (*C*) mRNA expression for cell type markers (lysozyme, mucin 2, CHGA) and transcription factors (*ATOH1*, *HES1*, and *NOTCH*, neurogenin 3) in lysates from Mut w DAPT or Mut (n = 4). The mRNA expression of lysozyme (n = 5), mucin 2 (n = 6), CHGA (n = 6), *Atoh1* (n = 5), and neurogenin 3 (n = 3) were increased upon treatment with DAPT, while expression of *HES1* and *NOTCH* (n = 6 in both cases) was not significantly changed. (*D*) Representative immunofluorescent images of CHGA for enteroendocrine cells (n = 4), lysozyme for Paneth Cells (n = 3), and bright field of PAS staining for goblet cells (n = 5) with quantification of cell types. Single-channel and nuclear stain images are represented in gray, while the overlay images are represented in color. Red asterisks denote the positive cells in the respective images. Increased number of goblet, Paneth, and enteroendocrine cells were found in DAPT-treated Mut enteroids when compared with untreated Mut enteroids. For immunofluorescent images, the white scale bar represents 250 μm, while the yellow scale bar represents 50 μm. For the bright-field image, the black scale bar denotes 200 μm, while the red scale bar denotes 100 μm. *$P < .05$, **$P < .01$, ***$P < .001$, ****$P < .0001$ by Student's t test for all results.
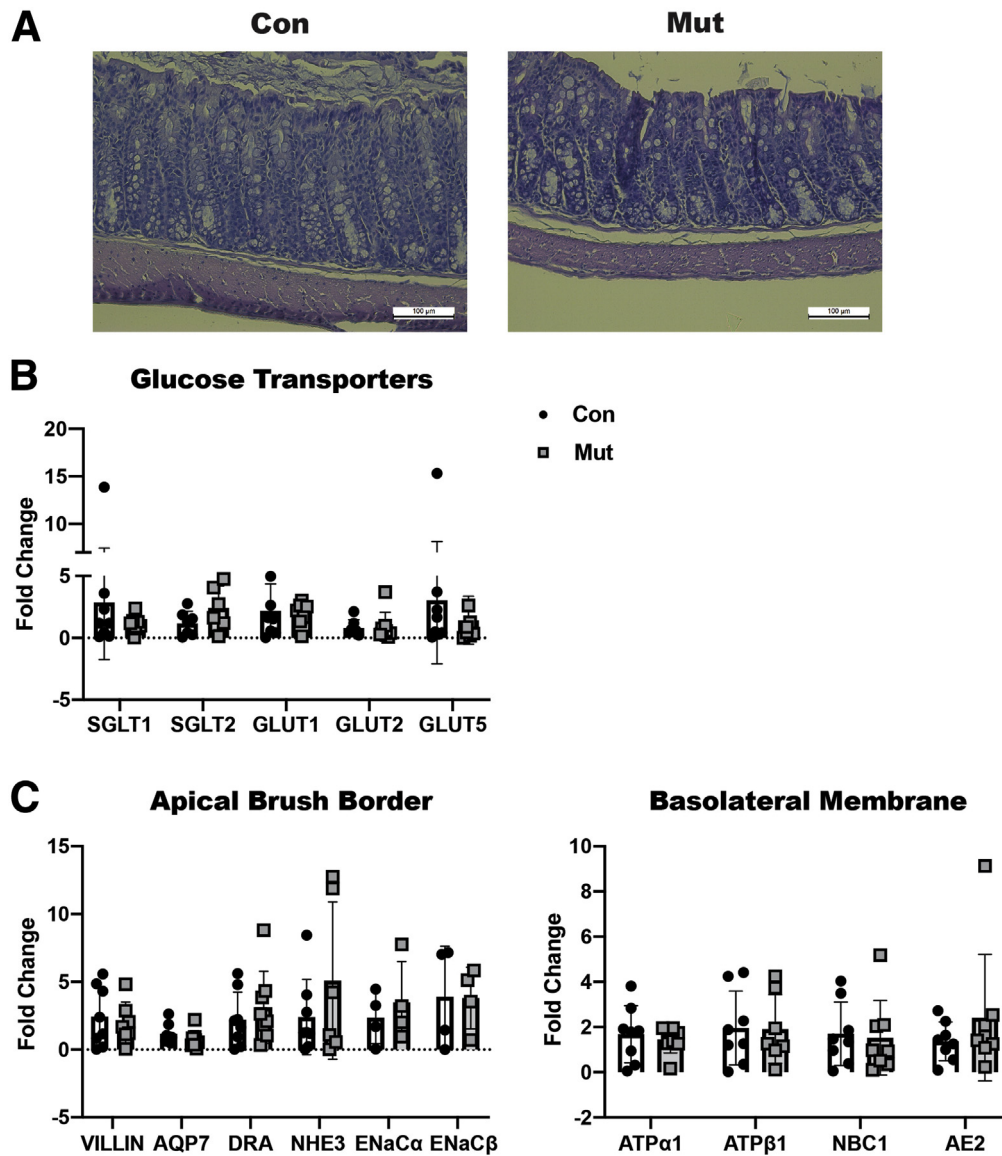
Figure 6. Unchanged colonic epithelial homeostasis in mutant mice. (*A*) Representative bright-field H&E staining images of colonic tissue section from control (Con) and mutant (Mut) mice (n = 4). Mild colonic cellular disorganization is noted along the brush border of the Mut tissue, although the overall architecture is preserved. Scale bar = 100 μm. (*B*) Equivalent mRNA expression for markers of glucose transporters sodium-glucose cotransporters 1 and 2 (*SGLT1*, *SGLT2*) *and* glucose transporters 1, 2, and 5 (*GLUT1*, *GLUT2*, *GLUT5*) in colonic tissue lysates of Mut mice when compared with Con mice (n = 6). (*C*) Equivalent mRNA expression for apical brush border markers *VILLIN*, aquaporin 7 (*AQP7*), downregulated in adenoma (*DRA*), sodium-hydrogen exchanger 3 (*NHE3*), and epithelial sodium channel alpha and beta (*ENaCα*, *ENaCβ*) as well as basolateral membrane markers ATPase beta 1 (*ATPβ1*) and ATPase alpha 1 (*ATPα1*), sodium bicarbonate cotransporter 1 (*NBC1*), and anion exchanger 2 (*AE2*) in colonic tissue lysates of Mut when compared with Con mice (n = 6).

brush border changes in the mutant mice might also suggest the involvement of altered cytoskeleton complexes in the mutant mice and may contribute to the defective expression of key brush border markers in the mutant mice. Moreover, we recently reported that endoplasmic reticulum stress and the UPR play a role in pathogenesis in mutant EPCAM mice.[43] Activation of UPR might lead to alterations in polarized absorptive enterocytes, which normally depend on intracellular transport of various components of the brush border for proper functioning.

In line with literature that emphasizes the role of defective enterocyte differentiation in other congenital diarrheal disorders,[25] the current study supports the contribution of aberrant IEC differentiation in the pathogenesis of CTE. Recent studies on MVID, another mucosal congenital diarrheal disease, revealed that differential expression of enterocyte apical transporters due to loss of the *MYO5B* gene contributes to disease, strongly suggesting apical enterocyte markers play an important role in congenital childhood diarrheal diseases.[23,24] The decreased

A

Figure 7. Unchanged epithelial homeostasis of pancreas in mutant mice. (*A*) Representative bright-field H&E staining images of pancreatic sections (acinar cells, islets of Langerhans, and interlobular ducts) from control (Con) and mutant (Mut) mice (n = 4). No changes in histology is noted between the groups. Scale bar = 100 μm. (*B*) Equivalent pancreatic lipase (n = 6) and amylase activity (n = 5) in blood serum of Con and Mut mice.

and inappropriate expression of NHE3, SGLT1, sucrase iso-maltase, and aquaporin 7 in the murine MVID model are consistent with our current findings in the CTE murine model; however, the expression of alkaline phosphatase was not decreased. On the other hand, expression of brush border hydrolases like lactase and maltase glucoamylase was decreased in the CTE model.

The present study revealed that the pathogenesis of CTE is affected by aberrant IEC differentiation in 2 ways. First, there is an alteration in the intestinal secretory lineage differentiation cascade due to increased Notch signaling pathways that ultimately lead to decreased Paneth cells, goblet cells, and enteroendocrine cells; and second, an increased number of absorptive epithelial cells are defective with reduced expression of key enterocyte membrane markers, perhaps related to their hypertrophy. Hence, the current study enhances our understanding of the

pathogenesis of CTE and the role of mutant EpCAM in the disease. There are currently neither cures nor directly targeted therapies for patients with this devastating disease, and thus understanding disease mechanisms is a necessary step toward improving disease outcomes. Future studies may also reveal how the cascade of mechanisms that regulate intestinal epithelial differentiation intersect with mutant EpCAM signaling pathways in CTE. Targeting of the biological processes uncovered here will lay the groundwork for the expansion of CTE therapeutics.

Materials And Methods
Animals

All animal experiments were performed according to the instructions and guidelines of, and were approved by, the University of California San Diego Institutional Animal Care

and Use Committee. Control C57BL/6N mice were obtained from Charles River Laboratories (Wilmington, MA). A previously described adult murine model with tamoxifen-inducible expression of mutant EpCAM was used for the current study (mutant).[7] Briefly, mice homozygous for the mutant EPCAM (deletion of EPCAM exon 4 construct),[6] in which the neomycin-resistant positive selection marker had been previously removed via Flp recombinase, were bred to B6.Cg-Tg(Cre/Esr1)5Amc/J mice obtained from the Jackson Laboratory (Bar Harbor, ME). This allowed for Cre-LoxP recombination and efficient deletion of exon 4 in EPCAM following administration of tamoxifen. Over the course of 5 days, mice were given tamoxifen on days 1 and 2 and had their weights measured daily. Studies were primarily performed on day 5 unless otherwise mentioned. In addition, littermates with wild-type EpCAM (control C57BL/6N) mice orally gavaged with tamoxifen served as control mice (control) for all experiments to exclude an effect of tamoxifen itself. Mice were studied between 9 and 14 weeks of age. All mice were euthanized using CO_2 gas asphyxiation in a CO_2 chamber followed by cervical dislocation. Both male and female mice were used in the study to avoid sex bias.

Enteroid Culture

Enteroid cultures were initiated, maintained, and expanded as previously described.[8] Briefly, enteroids from the proximal small intestinal crypts were isolated using collagenase I and cultured in Matrigel with 50% conditioned media (according to Miyoshi and Steppenbeck's large scale preparation using L-WRN cells)[46] containing ROCK inhibitors and Tgfβ inhibitors to form spheroids. For maintenance and expansion of the spheroids, the cultures were passaged every 2–3 days depending on spheroid size and density. For EDMs, enteroids were disrupted and plated on 6.5-mm Transwell inserts with 0.4-μm pores (Corning, Corning, NY) with 5% conditioned media for 2 days as described.[8] Then, 3 μM (Z) 4-hydroxytamoxifen (Cayman Chemical, Ann Arbor, MI) was added to the 5% conditioned media to generate CTE mutant EDM for the entire culture period. For inhibition of the Notch signaling pathway, 100 μM DAPT (AdipoGen Life Science, San Diego, CA) was added to the culture media simultaneously with tamoxifen treatment.

Stool Water Content

Fecal material from both control and mutant mice was collected on days 1, 3, and 5 (after TAM induction). Mice were held vertically until they spontaneously defecated. Feces were carefully placed in preweighed microcentrifuge tubes so that the stool remained undisturbed and the tubes were reweighed to obtain total fecal weight. In order to facilitate drying of the fecal material the microcentrifuge tubes were then placed in a heat block at 90°C overnight with the cap open. The tubes with dried feces were then reweighed to obtain dry weight. The percentage fecal water content was calculated by subtracting the dry fecal weight from the total fecal weight then dividing this value by the total fecal weight.

Oral Glucose Tolerance Test

All mice were fasted for 4 hours with free access to drinking water prior to being challenged with 2 g/kg of glucose by oral gavage, using 30% glucose prepared in drinking water. Blood was sampled via the tail vein at 0, 10, 30, and 90 minutes after glucose administration. Glucose concentration in blood was measured using a glucometer (Freestyle Lite, Abbott, Chicago, IL) and expressed as mg/dL.

Enzyme Activity Assay

Frozen duodenal tissue with luminal content was homogenized as follows. After weighing, the tissue was crushed with a plastic pestle in a 9-fold volume of phosphate-buffered saline (PBS) supplemented with protease inhibitors in a tube kept on ice. Following centrifugation at 3500 g for 10 minutes at 4°C, the supernatant was used for various assays and the protein content of the homogenate was measured using a DC protein assay kit (Bio-Rad, Hercules, CA). Lactase activity was assessed using a Lactase Assay Kit (Cat# E-BC-K131-S; Elabscience, Houston, TX) according to the manufacturer's instruction. Alkaline phosphatase activity was assessed using an alkaline phosphatase fluorometric assay kit (ab83371, Abcam, Cambridge, United Kingdom) according to the manufacturer's instruction. Maltase and sucrase activity were measured colorimetrically using the glucose oxidase peroxidase method with some modification of a published protocol.[47] Briefly, 10 μL of the tissue homogenate was added to 10 μL of the substrate (56 mM sucrose or maltose) and incubated for 1 hour at 37°C to generate glucose for generation of glucose. The quantity of glucose produced was then measured using a glucose assay kit (Sigma-Aldrich, St. Louis, MO; #GAGO20). For all assays, enzyme activity was normalized to total protein content. Pancreatic lipase and alpha amylase were evaluated from murine serum by enzyme-linked immunosorbent assay (ELISA) using Mouse Pancreatic Lipase ELISA kit (Cat# CSB-E16930m; CUSABIO, Houston, TX) and Mouse Pancreatic Alpha Amylase ELISA Kit (Cat# CSB-EL001689MO; CUSABIO) according to manufacturer's instruction. Briefly, the serum samples were diluted and both assays performed with respective biotin antibody followed by horseradish peroxidase–avidin and finally developed with kit provided TMB substrate. The optical density of the samples were measured at 450 nm and compared with the provided standards to calculate the quantity of the enzymes present in the serum.

Paraffin and Frozen Section Preparation

Intestinal jejunal tissue and distal colon and pancreatic tissue were fixed in 10% neutral buffered formalin (Thermo Fisher Scientific, Waltham, MA) containing zinc (for paraffin) or 4% paraformaldehyde (for frozen sections) overnight at 4°C and embedded in paraffin or Tissue-Tek Optimal Cutting Temperature (Sakura Finetek USA, Torrance, CA), respectively. Tissue for frozen sectioning was cryoprotected in a 30% sucrose solution (Macron, Center

Valley, PA) for an additional night at 4°C; 10-μm sections were utilized.

Histological Analysis

Histochemical study was performed from colon and pancreatic tissue of both control and mutant mice in order to evaluate whether mutant EpCAM affects the structure of the respective tissues. All histological analyses were performed using 5-μm sections of formalin buffer–fixed paraffin-embedded tissue using H&E staining as described previously.[6]

Immunofluorescent Staining

Immunofluorescent staining was performed in both intestinal tissue sections and EDMs. To stain intestinal sections, paraffin-embedded sections were deparaffinized and hydrated prior to blocking steps. Antigen retrieval was performed at pH 7 via microwave (VECTOR Antigen Unmasking Solution; Vector Labs, Burlingame, CA) before further processing. EDMs were cultured in Transwell inserts for lysozyme and chromogranin A staining. Cell monolayers were fixed with 4% paraforfaldehyde for 3 minutes. Both intestinal tissue and EDM samples were blocked in 5% goat serum in Tris-buffered saline (TBS) (tissue staining) or in PBS (EDM) for 1 hour at room temperature. Sections were incubated overnight with primary antibodies at 4°C in blocking buffer. Samples were then washed thrice for 5 minutes in TBS (tissue)/PBS (EDM) and incubated in Alexa Fluor 568 goat anti-rabbit antibodies (Thermo Fischer Scientific) for 1 hour at room temperature. Nuclei were stained using the Draq5 fluorescent probe (Thermo Fischer Scientific) in TBS (tissue staining)/PBS (EDM) and incubated for 10 minutes at room temperature. Finally, the samples were washed in PBS and mounted using Prolong Gold antifade reagent (Life Technologies, Eugene, OR). Slides were imaged using a Leica (Leica Microsystems, Buffalo Grove, IL) confocal imaging system (DMI4000 B) using a 25X Plan-Apo 0.8 numerical aperture with 40× objective lens. Images were captured using LASX v4.1 Image Acquisition software supplied by Leica. To evaluate the NICD expression in the murine intestinal tissue, the images were analyzed for fluorescence intensity. The average of mean gray value per area was calculated with ImageJ from 5 different areas per field. Four microscopic fields per sample were included in the study to determine the fluorescence intensity.

The primary antibodies used were as follows: NHE3 (GTX41967; GeneTex, Irvine, CA), Villin-1 (2369S; Cell Signaling Technology, Danvers, MA), Lysozyme (PA5-16668; Thermo Fisher Scientific), CHGA (ab15160; Abcam), NICD (07-1232; Millipore-Sigma).

IHC Staining

For immunohistochemical analysis of paraffin-embedded sections, endogenous peroxidase activity was blocked with a 3% H_2O_2 solution (VECTOR Antigen Unmasking Solution Citrate-based pH 6.0 H-3300; Vector Laboratories) prior to blocking with 5% goat serum (for CHGA) in TBS for 1 hour

at room temperature. The sections were then incubated with primary antibodies in blocking buffer overnight at 4°C. Samples were washed thrice for 5 minutes in TBS. After washing, slides were incubated with secondary antibodies for 30 minutes at room temperature. The signal was revealed using Vectastain Elite ABC-HRP kit and AEC Peroxidase (horseradish peroxidase) substrate 3-amino-9ethylcarbazole (VECTOR AEC Peroxidase Subtract Kit SK-4200; Vector Laboratories, Burlingame, CA). Samples were mounted using ProLong Gold antifade reagent (Life Technologies). Slides were imaged using a Leica (Leica Microsystems) inverted imaging system (DMi1) using a Hi Plan I 0.30 and 0.50 numerical aperture with 20× objective lens. Images were acquired at 20× magnification for enteroendocrine cell counts. Two representative images were taken of each section. All positively stained cells were counted within the image, followed by a count of all epithelial cells present within the image. The number of positively stained cells was then divided by total epithelial cells to generate a percentage of positive cells for one image, which was then averaged with the second image's percentage to create an average for each mouse.

Frozen sections were used for the immunohistochemical analysis of SGLT1. Slides were blocked in 5% rabbit serum and 1.5% bovine serum albumin (for SGLT1) in TBS containing 0.2% Triton X-100. The primary antibody was diluted in TBS containing 0.2% Triton X-100 overnight at 4°C. Samples were washed for 10 minutes 3 times in TBS containing 0.0005% Triton X-100. Slides were incubated in a goat secondary antibody for 30 minutes at room temperature. The signal was revealed using Vectastain Elite ABC-AP kit and alkaline phosphatase substrate (VECTOR Red Alkaline Phosphatase Substrate Kit SK-5100; Vector Laboratories). Samples were mounted using Prolong Gold antifade reagent (Life Technologies). Slides were imaged using Leica (Leica Microsystems) inverted imaging system (DMi1) using a Hi Plan I 0.30 and 0.50 Numerical aperture with 20× objective lens. The primary antibodies used were as follows: CHGA (ab15160; Abcam) and SGLT1 (EB09310; Everest Biotech, Oxfordshire, United Kingdom).

Electron Microscopy

Small intestinal tissue was collected from both control and mutant neonatal mice for electron microscopy as previously described.[6] Samples were prepared using modified Karnovsky's fixative[6] for at least 4 hours and processed according to protocol by University of California San Diego electron microscopy facility. Images were obtained at 4800× magnification, focusing on the brush border of the epithelial cells (enterocytes). To evaluate the brush border ultrastructure the mean of measurements from 6 different fields per sample were taken for analysis. In order to measure the microvilli height, an average of at least 8 properly oriented microvilli per field was obtained per sample. The height of the microvilli was measured using ImageJ 1.52K (National Institutes of Health, Bethesda, MD). Microvillus packing was measured by analysis of the

Table 1. Primer Sequences

Gene	Forward Primer (5′-3′)	Reverse Primer (5′-3′)
18s	GTAACCCGTTGAACCCCATT	CCATCCAATCGGTAGTAGCG
ATOH1	GTTGCGCTCACTCACAAATAAG	ACACAATAGTCGGTGTTCAGTAA
HNF1b	ACAATCCCCAGCAATCTCAGAA	GCTGCTAGCCACACTGTTAATGA
NOTCH	GCAACTGTCCTCTGCCATATAC	GTCTTCAGACTCCTTGCATACC
SOX9	GCAAGAACAAGCCACACGTC	TGTCCGTTCTTCACCGACTT
KLF4	ACCTGGCGAGTCTGACATGG	GGTCGTTGAACTCCTCGGTC
NEUG3	CTCACCATCCAAGTGTCCCC	GTTTGCTGAGTGCCAACTCG
HES1	CAACACGACACCGGACAAAC	CGGAGGTGCTTCACAGTCAT
NHE3	GCCTATGCCTTGGTGGTACT	CCGGCCATGTAGCTTCTCAT
DRA	AGGGAATGCTGATGCAGTTTGCTG	AGTTGAAATGCTACACTTGCCGCC
VILLIN	CTGGACCTTGGGAAGCTTATT	AAAGAGATCCGAGACCAGGA
AQP7	TTAACCACTTTGCAGGCGGA	TTCTTGTCGGTGATGGCGAA
NBC1	GGGGAAAGCCAAGTCCTACC	CCAGCAATCAGGTCGTGTCT
AE2	AACCTTCAGGAGCGAAGACG	TCTTCCTCACCAAGTGTCGC
ATPβ1	ACCGAGTGTTGGGCTTCAAA	GCACTGAACAGGCAGGACAT
ATPα1	TCCCCGGATTTCACAAACGA	CAGTGTACACGACGATGCCA
MGAM	TGAATTGGAAGACCTGGCCC	AGGCACAGGAGGAACGTCTG
LAC	TCAGGACTGCCCATCGACT	AAGGCACTGACATCAAACCCA
SI	ACTTACAGAGTTACTGGTGGCG	GGCATTGCTGGTCGTCCAAT
AP	GCCCGGTATGTTTGGAACCG	GGAAGGGTCTACTGAGGGGTT
FABP2	AGGAGCTGATTGCTGTCCGA	GAATCGCTTGGCCTCAACTC
CHGA	TGAGGATGAACTCTCAGAAGTGT	CTCTGTGGTTGCCTCAAAGC
LGR5	CTTCACTCGGTGCAGTGCT	GATCAGCCAGCTACCAAATAGG
BMI1	TTACGATGCCCAGCAGCAAT	AGGCAATGTCCATTAGCGTG
ASCL2	TCCAGTTGGTTAGGGGGCTA	CACTTGGCATTTGGTCAGGC
OLFM4	CAATGTCCTTAGCATTCGCCG	AAGGAGCGCTGATGTTCACC
PROM1	TGCTGGGAGGCAGAATAAAGG	CAGGGCATCCTTGGTCTGTT
MSI1	CTTCCTAGGGACCACAAGCC	CCTCCTCCCTGTTTCAGTGG
CDX2	TCAACCTCGCCACAACCTTCCC	TGGCTCAGCCTGGGATTGCT
MUC2	AATGACTTCACCACTCGGGAC	GGGTCTGGGTTGTGGCTTAC
LYSO	GAGACCGAAGCACCGACTAT	ATGCCTTGGGGATCTCTCAC
SGLT1	AGAAATACTGCGGCACACCA	GAGAGTACTGGCGCTGTTGA
SGLT2	ATCAGCCGCATTCTCTACCC	GATGTTAGAGCAGCCCACCT
GLUT1	ACCATCTTGGAGCTGTTCCG	GCCTTCTCGAAGATGCTCGT
GLUT2	ACCGGGATGATTGGCATGTT	GGACCTGGCCCAATCTCAAA
GLUT5	CCCGAAAAACCTACGAGGGG	CTGCGGGGACTCCAGTTAGA
ENaCα	TCGAGATGCTATCCTTGCAGA	GTGACAGAGGGAGACTCCGA
ENaCβ	TCCAGGCCTGTCTTCATTCCTGTT	TGGGAAGTCCCTGTTGTTGCAGTA

average number of properly oriented microvilli per unit length.

Periodic Acid-Schiff Staining

Periodic acid-Schiff (PAS) staining was performed to stain mucin-producing goblet cells in murine EDMs using a PAS Kit (Sigma-Aldrich) as described previously.[8] For PAS staining, EDMs were cultured in chamber slides in a fashion similar to that used for Transwell inserts. Briefly, EDMs in chamber slides were fixed with 4% paraformaldehyde for 3 minutes and stained with periodic acid for 1 minute, followed by Schiff's reagent for 5 minutes. The monolayer was then counterstained with hematoxylin for 1 minute. Scott's bluing reagent was used after hematoxylin staining in both cases. Cells that stained magenta were considered PAS positive for goblet cell counts.

Western Blotting

Intestinal tissue extracts were prepared by cell lysis using RIPA buffer (Cell Signaling Technology), followed by

centrifugation (14,000 g for 15 minutes) at 4°C. Proteins were resolved on a 4%–12% sodium dodecyl sulfate polyacrylamide gel electrophoresis gel, followed by transfer to a PVDF membrane (Immobilon-PSQ PVDF membrane; Millipore-Sigma, Burlington, MA). Immunoblotting was performed as described previously,[43] using rabbit polyclonal antibodies to HES1 (Thermo Fisher Scientific), MATH1 (ATOH1) (Developmental Studies Hybridoma Bank, Iowa City, IA), NHE3 (GTX41967; GeneTex), SGLT1 (EB09310; Everest Biotech) and GLUT2 (ab54460; Abcam), DRA (83545; Abcam), and villin (2369, Cell Signaling Technology). Mouse anti-β-Actin staining (A1978; Sigma-Aldrich) served as a loading control. The band intensities from the Western blot images were analyzed with ImageJ after normalizing for the loading control, and the fold change of protein expression in mutant models was calculated relative to the control group.

Quantative RT-PCR

Total mRNA for qRT-PCR studies of small intestine of control and mutant mice was isolated as per the manufacturer's instruction using a quick RNA micro prep kit (Zymo Research, Irvine, CA) as described previously.[8] First-strand complementary DNA was synthesized from 250 ng of total RNA with iScript cDNA Synthesis kit (Bio-Rad) following the manufacturer's protocol. The primers used for qRT-PCR in the current study are listed in Table 1. qRT-PCR reactions were set up using FastStart Universal SYBR Green Master Mix (Thermo Fisher Scientific) and thermal cycling was performed using a StepOnePlus (Applied Biosystems, Waltham, MA) Real-Time PCR System using Step One software v2.0 (Applied Biosystems). All qRT-PCR reactions were performed in duplicate. The relative fold change of the respective gene was calculated after normalization to the housekeeping gene (18s rRNA) and comparison with the control group.

Statistical Analysis

Data are presented for at least 3 biological replicates unless otherwise indicated. Error bars represent the SD of the mean of the measured parameter. The statistical significance of differences between the 2 groups was calculated by Student's unpaired t test (Prism 7; GraphPad Software, San Diego, CA). Two-tailed P values of $<.05$ were considered statistically significant. P values were designated as $P > .05$, $P < .05$, $P < .01$, and $P < .001$.

References

1. Goulet O, Salomon J, Ruemmele F, de Serres NP-M, Brousse N. Intestinal epithelial dysplasia (tufting enteropathy). Orphanet J Rare Dis 2007;2:20.
2. Reifen RM, Cutz E, Griffiths A-M, Ngan BY, Sherman PM. Tufting enteropathy: a newly recognized clinicopathological entity associated with refractory diarrhea in infants. J Pediatr Gastroenterol Nutr 1994; 18:379–385.
3. Sivagnanam M, Mueller JL, Lee H, Chen Z, Nelson SF, Turner D, Zlotkin SH, Pencharz PB, Ngan BY, Libiger O, Schork NJ, Lavine JE, Taylor S, Newbury RO, Kolodner RD, Hoffman HM. Identification of EpCAM as the gene for congenital tufting enteropathy. Gastroenterology 2008;135:429–437.
4. Pathak SJ, Mueller JL, Okamoto K, Das B, Hertecant J, Greenhalgh L, Cole T, Pinsk V, Yerushalmi B, Gurkan OE, Yourshaw M, Hernandez E, Oesterreicher S, Naik S, Sanderson IR, Axelsson I, Agardh D, Boland CR, Martin MG, Putnam CD, Sivagnanam M. EPCAM mutation update: Variants associated with congenital tufting enteropathy and Lynch syndrome. Hum Mutat 2019; 40:142–161.
5. Guerra E, Lattanzio R, La Sorda R, Dini F, Tiboni GM, Piantelli M, Alberti S. mTrop1/Epcam knockout mice develop congenital tufting enteropathy through dysregulation of intestinal E-cadherin/β-catenin. PLoS One 2012;7:e49302.
6. Mueller JL, McGeough MD, Pena CA, Sivagnanam M. Functional consequences of EpCam mutation in mice and men. Am J Physiol Gastrointest Liver Physiol 2014; 306:G278–G288.
7. Kozan PA, McGeough MD, Peña CA, Mueller JL, Barrett KE, Marchelletta RR, Sivagnanam M. Mutation of EpCAM leads to intestinal barrier and ion transport dysfunction. J Mol Med 2015;93:535–545.
8. Das B, Okamoto K, Rabalais J, Kozan PA, Marchelletta RR, McGeough MD, Durali N, Go M, Barrett KE, Das S, Sivagnanam M. Enteroids expressing a disease-associated mutant of EpCAM are a model for congenital tufting enteropathy. Am J Physiol Gastrointest Liver Physiol 2019;317:G580–G591.
9. Barth AIM, Kim H, Riedel-Kruse IH. Regulation of epithelial migration by epithelial cell adhesion molecule requires its Claudin-7 interaction domain. PLoS One 2018;13:e0204957.
10. Salomon J, Gaston C, Magescas J, Duvauchelle B, Canioni D, Sengmanivong L, Mayeux A, Michaux G, Campeotto F, Lemale J, Viala J, Poirier F, Minc N, Schmitz J, Brousse N, Ladoux B, Goulet O, Delacour D. Contractile forces at tricellular contacts modulate epithelial organization and monolayer integrity. Nat Commun 2017;8:13998.
11. Lei Z, Maeda T, Tamura A, Nakamura T, Yamazaki Y, Shiratori H, Yashiro K, Tsukita S, Hamada H. EpCAM contributes to formation of functional tight junction in the intestinal epithelium by recruiting claudin proteins. Dev Biol 2012;371:136–145.
12. Wu C-J, Feng X, Lu M, Morimura S, Udey MC. Matriptase-mediated cleavage of EpCAM destabilizes claudins and dysregulates intestinal epithelial homeostasis. J Clin Invest 2017;127:623.
13. Noah TK, Donahue B, Shroyer NF. Intestinal development and differentiation. Exp Cell Res 2011; 317:2702–2710.
14. Fre S, Huyghe M, Mourikis P, Robine S, Louvard D, Artavanis-Tsakonas S. Notch signals control the fate of immature progenitor cells in the intestine. Nature 2005; 435:964–968.

15. Kim TH, Shivdasani RA. Genetic evidence that intestinal Notch functions vary regionally and operate through a common mechanism of Math1 repression. J Biol Chem 2011;286:11427–11433.

16. Shroyer NF, Helmrath MA, Wang VY, Antalffy B, Henning SJ, Zoghbi HY. Intestine-specific ablation of mouse atonal homolog 1 (Math1) reveals a role in cellular homeostasis. Gastroenterology 2007;132:2478–2488.

17. Zecchini V, Domaschenz R, Winton D, Jones P. Notch signaling regulates the differentiation of post-mitotic intestinal epithelial cells. Genes Dev 2005;19:1686–1691.

18. Canani RB, Terrin G. Recent progress in congenital diarrheal disorders. Curr Gastroenterol Rep 2011; 13:257–264.

19. Kuokkanen M, Kokkonen J, Enattah NS, Ylisaukko-Oja T, Komu H, Varilo T, Peltonen L, Savilahti E, Jarvela I. Mutations in the translated region of the lactase gene (LCT) underlie congenital lactase deficiency. Am J Hum Genet 2006;78:339–344.

20. Martin MG, Turk E, Lostao MP, Kerner C, Wright EM. Defects in Na+/glucose cotransporter (SGLT1) trafficking and function cause glucose-galactose malabsorption. Nat Genet 1996;12:216–220.

21. Ritz V, Alfalah M, Zimmer KP, Schmitz J, Jacob R, Naim HY. Congenital sucrase-isomaltase deficiency because of an accumulation of the mutant enzyme in the endoplasmic reticulum. Gastroenterology 2003; 125:1678–1685.

22. Wedenoja S, Pekansaari E, Hoglund P, Makela S, Holmberg C, Kere J. Update on SLC26A3 mutations in congenital chloride diarrhea. Hum Mutat 2011; 32:715–722.

23. Engevik AC, Kaji I, Engevik MA, Meyer AR, Weis VG, Goldstein A, Hess MW, Muller T, Koepsell H, Dudeja PK, Tyska M, Huber LA, Shub MD, Ameen N, Goldenring JR. Loss of MYO5B leads to reductions in Na(+) absorption with maintenance of CFTR-dependent Cl(-) secretion in enterocytes. Gastroenterology 2018;155:1883–1897.e10.

24. Kravtsov DV, Ahsan MK, Kumari V, van Ijzendoorn SC, Reyes-Mugica M, Kumar A, Gujral T, Dudeja PK, Ameen NA. Identification of intestinal ion transport defects in microvillus inclusion disease. Am J Physiol Gastrointest Liver Physiol 2016;311:G142–G155.

25. Overeem AW, Posovszky C, Rings EH, Giepmans BN, van IJzendoorn SC. The role of enterocyte defects in the pathogenesis of congenital diarrheal disorders. Dis Model Mech 2016;9:1–12.

26. Yan KS, Chia LA, Li X, Ootani A, Su J, Lee JY, Su N, Luo Y, Heilshorn SC, Amieva MR, Sangiorgi E, Capecchi MR, Kuo CJ. The intestinal stem cell markers Bmi1 and Lgr5 identify two functionally distinct populations. Proc Natl Acad Sci U S A 2012; 109:466–471.

27. Baker M. Intestinal stem cells: one gene to rule them all. Nat Rep Stem Cells 2009 Mar 12 [E-pub ahead of print].

28. van der Flier LG, Haegebarth A, Stange DE, van de Wetering M, Clevers H. OLFM4 is a robust marker for stem cells in human intestine and marks a subset of colorectal cancer cells. Gastroenterology 2009; 137:15–17.

29. Snippert HJ, van Es JH, van den Born M, Begthel H, Stange DE, Barker N, Clevers H. Prominin-1/CD133 marks stem cells and early progenitors in mouse small intestine. Gastroenterology 2009;136:2187–2194.e1.

30. Potten CS, Booth C, Tudor GL, Booth D, Brady G, Hurley P, Ashton G, Clarke R, Sakakibara S, Okano H. Identification of a putative intestinal stem cell and early lineage marker; musashi-1. Differentiation 2003; 71:28–41.

31. Saad RS, Ghorab Z, Khalifa MA, Xu M. CDX2 as a marker for intestinal differentiation: Its utility and limitations. World J Gastrointest Surg 2011;3:159–166.

32. Yang Q, Bermingham NA, Finegold MJ, Zoghbi HY. Requirement of Math1 for secretory cell lineage commitment in the mouse intestine. Science 2001; 294:2155–2158.

33. Demitrack ES, Samuelson LC. Notch regulation of gastrointestinal stem cells. J Physiol 2016;594: 4791–4803.

34. Grenov B, Briend A, Sangild PT, Thymann T, Rytter MH, Hother AL, Molgaard C, Michaelsen KF. Undernourished children and milk lactose. Food Nutr Bull 2016;37:85–99.

35. Gambarara M, Diamanti A, Ferretti F, Papadatou B, Knafelz D, Pietrobattista A, Castro M. Intractable diarrhea of infancy with congenital intestinal mucosa abnormalities: outcome of four cases. Transplant Proc 2003;35:3052–3053.

36. Kahvecioglu D, Yildiz D, Kilic A, Ince-Alkan B, Erdeve O, Kuloglu Z, Atasay B, Ensari A, Yilmaz R, Arsan S. A rare cause of congenital diarrhea in a Turkish newborn: tufting enteropathy. Turk J Pediatr 2014;56:440–443.

37. Rehfeld JF. A centenary of gastrointestinal endocrinology. Horm Metab Res 2004;36:735–741.

38. Latorre R, Sternini C, De Giorgio R, Greenwood-Van Meerveld B. Enteroendocrine cells: a review of their role in brain-gut communication. Neurogastroenterol Motil 2016;28:620–630.

39. Wang J, Cortina G, Wu SV, Tran R, Cho JH, Tsai MJ, Bailey TJ, Jamrich M, Ament ME, Treem WR, Hill ID, Vargas JH, Gershman G, Farmer DG, Reyen L, Martin MG. Mutant neurogenin-3 in congenital malabsorptive diarrhea. N Engl J Med 2006;355:270–280.

40. Lo YH, Chung E, Li Z, Wan YW, Mahe MM, Chen MS, Noah TK, Bell KN, Yalamanchili HK, Klisch TJ, Liu Z, Park JS, Shroyer NF. Transcriptional regulation by ATOH1 and its target SPDEF in the intestine. Cell Mol Gastroenterol Hepatol 2017;3:51–71.

41. Pearce SC, Al-Jawadi A, Kishida K, Yu S, Hu M, Fritzky LF, Edelblum KL, Gao N, Ferraris RP. Marked differences in tight junction composition and macromolecular permeability among different intestinal cell types. BMC Biol 2018;16:19.

42. Heijmans J, van Lidth de Jeude JF, Koo BK, Rosekrans SL, Wielenga MC, van de Wetering M, Ferrante M, Lee AS, Onderwater JJ, Paton JC, Paton AW, Mommaas AM, Kodach LL, Hardwick JC, Hommes DW, Clevers H, Muncan V, van den Brink GR. ER stress causes rapid loss of intestinal epithelial stemness through activation of the unfolded protein response. Cell Rep 2013;3:1128–1139.

43. Das B, Okamoto K, Rabalais J, Marchelletta RR, Barrett KE, Das S, Niwa M, Sivagnanam M. Congenital tufting enteropathy-associated mutant of epithelial cell adhesion molecule activates the unfolded protein response in a murine model of the disease. Cells 2020;9:946.

44. Huang L, Yang Y, Yang F, Liu S, Zhu Z, Lei Z, Guo J. Functions of EpCAM in physiological processes and diseases (Review). Int J Mol Med 2018;42:1771–1785.

45. Donowitz M, Cha B, Zachos NC, Brett CL, Sharma A, Tse CM, Li X. NHERF family and NHE3 regulation. J Physiol 2005;567:3–11.

46. Miyoshi H, Stappenbeck TS. In vitro expansion and genetic modification of gastrointestinal stem cells in spheroid culture. Nat Protoc 2013;8:2471–2482.

47. Dahlqvist A. Assay of intestinal disaccharidases. Anal Biochem 1968;22:99–107.

Correspondence
Address correspondence to: Mamata Sivagnanam, MD, Division of Gastroenterology, Hepatology and Nutrition, Department of Pediatrics, 9500 Gilman Drive, La Jolla, CA 92093. e-mail: mengineer@health.ucsd.edu; fax: 858-967-8917.